Structure and mechanical properties of artificial protein hydrogels assembled through aggregation of leucine zipper peptide domains

Wei Shen, Julia A. Kornfield* and David A. Tirrell*

Received 31st July 2006, Accepted 20th October 2006
First published as an Advance Article on the web 9th November 2006
DOI: 10.1039/b610986a

Artificial protein hydrogels made from a triblock protein (designated $AC_{10}A$, where A is an acidic zipper domain and C_{10} comprises 10 repeats of the nonapeptide sequence —(AG)$_3$PEG—) exhibit normalized plateau storage moduli (G'_∞/nkT) less than 0.13 at all concentrations, pH values, and ionic strengths examined. These gels are surprisingly soft due to loop formation at the expense of bridges between physical junctions. Molecular-level evidence of loop formation is provided by strong fluorescence energy transfer (FRET) between distinct chromophores placed at the C- and N-termini of labelled chains diluted in an excess of unlabelled chains. The tendency to form loops originates from the compact size of the random coil midblock (mean $R_{H(C10)} \approx 20$ Å, determined from quasi-elastic light scattering of C_{10}), and is facilitated by the ability of the leucine zipper domains to form antiparallel aggregates. Although the aggregation number of the leucine zipper domains is small (tetrameric, determined from multi-angle static light scattering of AC_{10} diblock), the average center-to-center distance between aggregates is roughly 1.5 times the average end-to-end distance of the C_{10} domain in a 7% w/v network. To avoid stretching the C_{10} domain, the chains tend to form loops. Changes in pH or ionic strength that expand the polyelectrolyte midblock favor bridging, leading to greater G'_∞ as long as leucine zipper endblocks do not dissociate. Understanding of the network structure provided successful design strategies to increase the rigidity of these hydrogels. In contrast to intuitive design concepts for rubber and gel materials, it was shown that increasing either the length or the charge density of the midblock increases rigidity, because fewer chains are wasted in loop formation.

Introduction

The genetically engineered multidomain protein $AC_{10}A$, which consists of two associative leucine zipper endblocks (A) and a random coil midblock (C_{10}), self-assembles into solid-like hydrogels characteristic of a storage modulus (G') exhibiting a pronounced plateau extending to times at least of the order of seconds and of a loss modulus (G'') that is much smaller than G' in the plateau region.[1] These artificial protein hydrogels introduced a new class of engineered biomaterials.[2] The flexibility of recombinant DNA technology allows biological information—including cell binding domains and enzyme recognition sites—to be programmed into designed macromolecules. Protein hydrogels are promising candidates for use in biomedical applications such as controlled release, cell immobilization, and tissue engineering that demand specific combinations of biological and physical properties. For example, it has been shown that both cell adhesion ligands[3–5] and rigidity of scaffold materials[6–9] are critical extracellular signals that regulate cell adhesion, spreading, migration, and even survival. Therefore, control of viscoelastic properties and the underlying structure[10] and dynamics[11,12] is central to applications of protein hydrogels. The viscoelastic properties of artificial protein gels are governed by the structure of the network they assemble[10] and the dynamics of exchange of endblocks between the physical junctions of the network.[11] Structural aspects of the network include the number of leucine zippers per cluster, the orientation of the zippers with respect to each other in the cluster, and the ratio of midblock "bridges" (connecting different clusters) to "loops" (both ends in the same cluster). These can be tuned by molecular design of the specific leucine zipper domain(s)[10] and the random coil domain. Here, we examine the structure of the network and its dependence on the length and charge density of the random coil domain. We investigated the rigidity (storage modulus) of $AC_{10}A$ gels under various conditions of pH, concentration, and ionic strength by oscillatory shear measurements. The molecular basis of the macroscopic material properties was also examined and molecular design strategies to increase the rigidity of protein hydrogels were identified.

Division of Chemistry and Chemical Engineering, California Institute of Technology, Pasadena, California 91125, USA.
E-mail: jak@cheme.caltech.edu; tirrell@caltech.edu; weishen@its.caltech.edu; Fax: +1 (626) 568-8743; Fax: +1 (626) 793-8472; Tel: +1 (626) 395-4138 Tel: +1 (626) 395-3140

Experimental

Protein synthesis and purification

Fig. 1 shows the amino acid sequences of the proteins used in this study, including $AC_{10}A$, model polypeptides for the zipper (A) and random-coil (C) domains, polypeptides used for fluorescence labeling studies, and polypeptides with varied charge density and length of the random-coil domain. Genes

$AC_{10}A_{trp}$ ($AC_{10}A$): MR**[6H]**DDDDKA**[A]**IGDHVAPRDTSYRDPMG**[C_{10}]**ARMPT**[A]**IGDHVAPRDTSW

$_{trp}AC_{10}A_{cys}$: MR**[6H]**DDDDKWA**[A]**IGDHVAPRDTSYRDPMG**[C_{10}]**ARMPT**[A]**IGDHVAPRDTSMGGC

$AC_{10}A_{no\text{-}trp}$: MR**[6H]**MA**[A]**IGDLNNTSYRDPMG**[C_{10}]**ARMPT**[A]**IGDLNNTSGIRRPAAKLN

$_{trp}A_{cys}$: MR**[6H]**DDDDKWA**[A]**IGDHVAPRDTSMGGC

A_{trp}: MR**[6H]**DDDDKASYR**[A]**IGDPRMPTSW

$_{cys}A$: MC**[6H]**DDDDKASYR**[A]**IGDPRMPTSW

C_{10trp}: MR**[6H]**DDDDKASYRDPMG**[C_{10}]**ARMPTSW

$C_{10}A_{cys}$: MR**[6H]**DDDDKWASYRDPMG**[C_{10}]** ARMPT**[A]**IGDHVAPRDTSMGGC

AC_{10trp}: MR**[6H]**DDDDKA**[A]**IGDHVAPRDTSYRDPMG**[C_{10}]**ARMPTSW

$AC_{26}A_{trp}$: MR**[6H]**DDDDKA**[A]**IGDHVAPRDTSYRDPMG**[C_{26}]**ARMPT**[A]**IGDHVAPRDTSW

$AC^*_{18}A_{trp}$: MR**[6H]**DDDDKA**[A]**IGDHVAPRDTSYRDPMG**[C^*_{18}]**ARMPT**[A]**IGDHVAPRDTSW

Abbreviation for domains:
[6H]: GSHHHHHHGS
[A]: S(or D)GDLENEVAQLEREVRSLEDEAAELEQKVSRLKNEIEDLKAE
[C_{10}]: $[AGAGAGPEG]_{10}$
[C_{26}]: $[AGAGAGPEG]_{26}$
[C^*_{18}]: $[AGPEG]_{18}$

Fig. 1 Amino acid sequences of proteins.

encoding these proteins were designed and cloned into expression vector pQE9 (Qiagen, Chatsworth, CA), by using standard recombinant DNA technology. Expression vectors were transformed into *Escherichia coli* strain SG13009, which carries the repressor plasmid pREP4 (Qiagen, Chatsworth, CA). Proteins were expressed and purified as described previously.[13] Typical protein yields were 60–100 mg per litre of cell culture.

Rheological measurements

Protein was dissolved in phosphate buffer (13 mM $NaH_2PO_4{\cdot}H_2O$, 87 mM $Na_2HPO_4{\cdot}7H_2O$) with 0.5% sodium azide. Initially the pH was low ($\sim$4.5) and the protein was insoluble. As NaOH was added and the pH approached 7, the sample became a transparent gel. The time between sample preparation and rheological measurements varied up to 24 hours. No systematic variation with aging time was observed over this time range. Visually, samples remained stable as gels for months. Prior to loading on the rheometer, each sample was centrifuged to remove entrapped bubbles. Measurements were performed using an RFS III rheometer (TA Instruments, New Castle, Delaware) at a temperature of 22.0 $\pm$ 0.1 °C, controlled by a Peltier thermoelectric device. A cone-and-plate geometry (0.04 rad cone angle and 25 mm diameter) was used to acquire dynamic mechanical spectra from 100 rad s^{-1} to 0.001 rad s^{-1}. To reduce the sample size, a parallel-plate geometry (0.5 mm gap and 8 mm diameter) was used for frequency sweep measurements from 100 rad s^{-1} to 1 rad s^{-1} to determine the plateau storage modulus. The edge of each sample was covered with mineral oil to minimize solvent evaporation. All frequency sweep measurements were performed at 1% strain, which was confirmed to be within the linear viscoelastic regime from strain sweep tests. The measurement error of the plateau storage modulus is smaller than $\pm$3.5%, as revealed by at least triplicate measurements for 7% $AC_{10}A$ gels prepared at various pH values.

Fluorescence labeling

Coumarin was site-specifically ligated to the cysteine residues engineered at the C-termini of $_{trp}A_{cys}$ and $_{trp}AC_{10}A_{cys}$. Protein solutions (100 μM) were prepared in phosphate buffer (10 mM NaH_2PO_4, 90 mM NaCl). A tris(2-carboxyethyl)phosphine hydrochloride (TCEP) (Pierce, Rockford, IL) stock solution (100 mM) was added to each protein solution to a final concentration of 2 mM. The pH of the mixture was adjusted to 4.5, and the solution was incubated at room temperature for 30 min to allow reduction of disulfide bonds. The pH was adjusted to 6.5. A 7-diethylamino-3-(4′-maleimidylphenyl)-4-methylcoumarin (CPM, Molecular Probes, Eugene, OR) stock solution (100 mM) was freshly prepared in DMSO, and added to each reduced protein solution to a concentration of 1 mM. The mixture was incubated in the dark at room temperature for 30 min. Additional labeling reagent (10 moles of CPM per mole of protein) was added, and the mixture was incubated for an additional 30 min. The sample was concentrated from 10 mL to 1 mL in a Centricon YM-3 centrifugal filter unit (molecular weight cutoff 3000, Millipore, Billerica, MA), and subjected to gel filtration on a Sephadex G-25 (Amersham

Biosciences, Piscataway, NJ) column (1.5 cm diameter × 30 cm height) to remove unreacted dye. The protein fraction was collected, dialyzed against sterile deionized water, and lyophilized in the dark. The signals corresponding to unmodified chains in the MALDI mass spectra of the proteins (sinapinic acid matrix) were almost eliminated by this procedure. The absorbance at 387 nm (Cary 50 Bio UV–vis spectrophotometer, Varian, Palo Alto, CA) showed *ca.* 83% of $_{trp}A_{cys}$ and *ca.* 70% of $_{trp}AC_{10}A_{cys}$ were labelled, respectively, using an extinction coefficient of 28 000 M^{-1} cm^{-1} for CPM.[14]

The same method was used to ligate coumarin to the thiol group of polyethylene glycol mPEG-SH (molecular weight 5000, Nektar Therapeutics).

Fluorescence measurements

Solutions of $_{trp}A_{cys}$ and the coumarin-modified protein $_{trp}A_{cys}$-CPM were each prepared in 100 mM phosphate buffer (pH 7.6) at a concentration of 100 μM. The solutions were subjected to fluorescence measurements on a fluorometer (Photon Technology International, Inc., Lawrenceville, NJ) at an excitation wavelength of 300 nm. Emission scans from 308 nm to 590 nm were recorded.

Solutions containing *ca.* 1% w/v triblock protein at a ratio of labelled to unlabelled chains of 1 : 25 were made as follows. Appropriate controls were also prepared. A solution of the unlabelled chain $AC_{10}A_{no\text{-}trp}$ was prepared in 100 mM phosphate buffer (pH 7.6) at a concentration of 1.25%. Stock solutions of the labelled chains $_{trp}AC_{10}A_{cys}$, $_{trp}AC_{10}A_{cys}$-CPM, and PEG-CPM were individually added to the $AC_{10}A_{no\text{-}trp}$ solution to yield samples in which the ratio of labelled to unlabelled chains was 1 : 25. The concentration of $AC_{10}A_{no\text{-}trp}$ was 1.01% after mixing. Samples were subjected to fluorescence measurements on a fluorometer (Photon Technology International, Inc., Lawrenceville, NJ) at an excitation wavelength of 300 nm. Emission scans from 308 nm to 590 nm were recorded.

Quasi-elastic light scattering

Quasi-elastic light scattering measurements on a pH 10.0, 140 μM C_{10trp} solution were performed with WyattQELS (Wyatt Technology Corporation, CA) and BI-9000AT (Brookhaven, NY) digital autocorrelators to characterize correlation times from 1 μs to 60 μs, and from 10 μs to 20 000 μs, respectively. Because contaminant particles that passed through 0.2 μm pore filters added a long-time tail to the correlation function, the long-time data were obtained from solutions that had been filtered through 0.02 μm pore size filters. The correlation function was analyzed with software (based on the CONTIN algorithm) provided by Brookhaven.

Multi-angle static light scattering

Solutions of AC_{10trp} were prepared in 100 mM phosphate buffer (pH 7.6) at concentrations of 0.179 mg mL^{-1}, 0.362 mg mL^{-1}, 0.540 mg mL^{-1}, and 0.721 mg mL^{-1} by weighing at least 3 mg of the protein on a microbalance with an error less than 0.05 mg. The solutions were each filtered through a 0.2 μm pore size filter (polysulfone membrane, Pall Corporation). The protein concentration did not change after filtration, confirmed by the absorbance at 280 nm measured on a Cary 50 Bio ultraviolet–visible spectrophotometer (Varian, Palo Alto, California). The filtered solutions were subjected to multi-angle light scattering measurements on a DAWN EOS light scattering instrument (Wyatt Technology Corporation) at an operating wavelength of 690 nm. The light scattering at detector angles (θ) of 39.8, 45.0, 51.3, 59.0, 68.2, 78.7, 90.0, 101.3, 111.8, 121.0, 128.7, 135.0, 140.2, 144.5 were analyzed by using the Zimm formalism and a dn/dc value of 0.185.[15]

Electrophoretic assessment of parallel *vs.* antiparallel leucine zipper association

Solutions of $_{cys}A$ and $C_{10}A_{cys}$ were prepared in 100 mM phosphate buffer at a concentration of 100 μM and mixed in a volumetric ratio of 1 : 1. The pH of the mixture was adjusted to 8.0, and the sample was incubated at room temperature under air for 48 h. A redox buffer (125 μM reduced glutathione, 62.5 μM oxidized glutathione, 1 M NaCl, 50 mM MOPS, pH 7.5)[16] was then added into the mixture in a volumetric ratio of 1 : 1. The sample was incubated at room temperature for 3 h and subjected to electrophoresis on a 12% denaturing polyacrylamide gel (PAGE) using the standard protocol with dithiothreitol omitted from the sample buffer. The gel was stained with Coomassie Brilliant Blue R250. Densitometry analysis was used to determine the relative intensities of protein bands using NIH ImageJ (http://rsb.info.nih.gov/ij/).

Results

Plateau storage modulus of artificial protein hydrogels

The linear viscoelastic regime for $AC_{10}A$ hydrogels extends up to 10% strain according to strain sweep tests. Within the linear regime, these hydrogels exhibit a high-frequency plateau in the storage modulus (nearly constant $G' \approx G'_\infty$, where G'_∞ is the plateau storage modulus) and a pronounced peak in the loss modulus G'' near the frequency where G' and G'' cross (ω_x, indicative of a characteristic relaxation time $\tau_r \sim 1/\omega_x$). At lower frequency the dynamic moduli approach terminal behavior ($G' \sim \omega^2$ and $G'' \sim \omega$)[17] (Fig. 2).

G'_∞ of $AC_{10}A$ hydrogels increases nonlinearly with concentration (Fig. 3). The normalized plateau storage modulus G'_∞/nkT (nkT is the modulus of an ideal network of n chains per unit volume in which 100% chains are elastically effective) is much less than 1: even at a concentration of 9% w/v, the value of G'_∞/nkT is only *ca.* 0.13. With increasing concentration, G'_∞/nkT increases, suggesting that network topology changes with concentration.

G'_∞ varies nonmonotonically with pH between 7 and 10 (Fig. 4). For 7% w/v $AC_{10}A$ hydrogels, G'_∞ increases with pH between 7 and 8, then levels off at a maximum G'_∞/nkT that is less than 0.07, and starts to decline at pH values above 9.0.

G'_∞ of $AC_{10}A$ hydrogels decreases with increasing ionic strength (Fig. 5).

In contrast to the behavior of conventional networks, increasing the length of the midblock causes the modulus to increase: when the C_{10} midblock (90 amino acids) is replaced

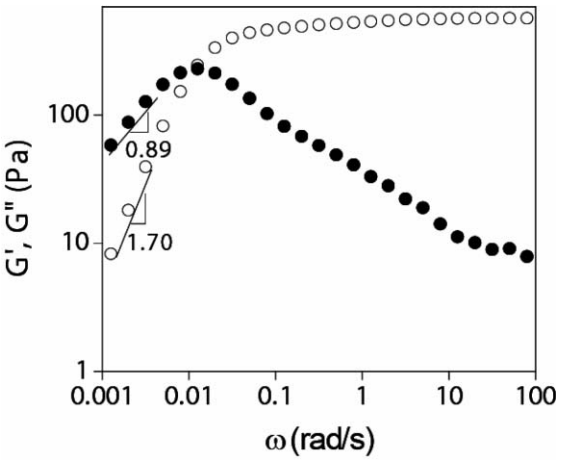

Fig. 2 Dynamic moduli of an $AC_{10}A$ hydrogel. (7% w/v, pH 8.0, 100 mM phosphate buffer, 22 °C) ○ G'; ● G''.

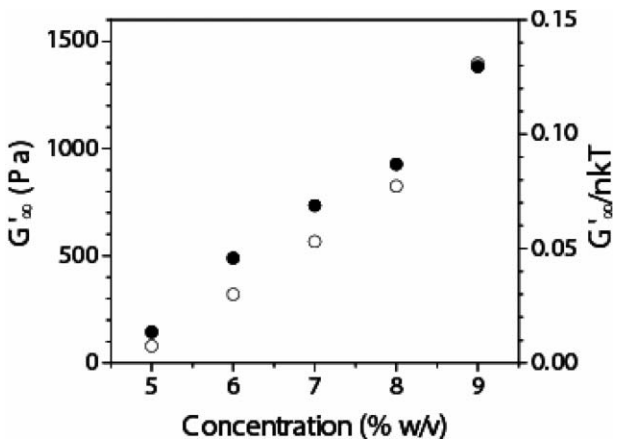

Fig. 3 Concentration dependence of plateau storage modulus of $AC_{10}A$ hydrogels (pH 8.0, 100 mM phosphate buffer, 22 °C) ○ G'_∞; ● G'_∞/nkT.

by C_{26} (234 amino acids), G'_∞ of the resulting hydrogel increases 1.7 fold at the same weight concentration (7% w/v), corresponding to an even greater (2.4 fold) increase in G'_∞/nkT (Fig. 6). Increasing the charge density on the midblock while keeping its contour length fixed also increases G'_∞: when the midblock C_{10} (containing 10 charged residues when fully deprotonated) is replaced by C^*_{18} (containing 18 charged residues when fully deprotonated), G'_∞ doubles (Fig. 6).

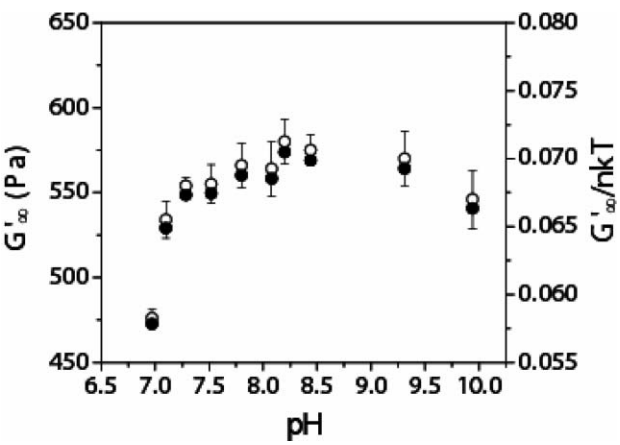

Fig. 4 Effect of pH on plateau storage modulus of $AC_{10}A$ hydrogels. (7% w/v, 100 mM phosphate buffer, 22 °C) ○ G'_∞; ● G'_∞/nkT.

Fluorescence resonance energy transfer

Fluorescence resonance energy transfer (FRET) was used to examine two aspects of network topology: the local arrangement of leucine zipper strands within their aggregates (relative preference for parallel *vs.* antiparallel orientation) and the configuration of triblock chains in the network (relative preference for looped *vs.* bridged states). We used a tryptophan–coumarin donor–acceptor pair, which has a Föster distance of 31 Å[18] and which has been used extensively to probe structure and interactions of biopolymers.[19,20] Fluorescence from isolated tryptophan is observed between 308 and 410 nm; energy transfer to coumarin causes the appearance of a new emission maximum near 475 nm. Since the Föster distance for the tryptophan–coumarin pair is significantly shorter than the length of the leucine zipper domain (65 Å),[21] energy transfer from a tryptophan chromophore to a coumarin at the opposite end of a given strand is negligible.

A doubly labelled leucine zipper peptide ($_{trp}A_{cys}$-CPM) was prepared with tryptophan genetically engineered at the N-terminus of the isolated A domain, and coumarin ligated to the C-terminal cysteine. In micromolar solutions of $_{trp}A_{cys}$-CPM, the tryptophan fluorescence was strongly quenched (Fig. 7a). The quenching efficiency was estimated to be 85–90% ($E = 1 - (F_{DA}/F_D)$, where F_{DA} and F_D are the donor fluorescence in the presence and absence of the acceptor, respectively; fluorescence intensities were based on the areas of the tryptophan emission peaks between 308 and 410 nm). Quenching appears not to result from random collision of peptide aggregates, since the quenching efficiency is insensitive to concentration (Fig. 7b). This leads to the conclusion that N-terminal tryptophan residues are brought into proximity with C-terminal coumarin chromophores of neighboring leucine zipper strands within the aggregates, which suggests antiparallel strand orientation.

The FRET technique was also used to probe the formation of intramolecular loops in $AC_{10}A$ solutions. If $AC_{10}A$ chains

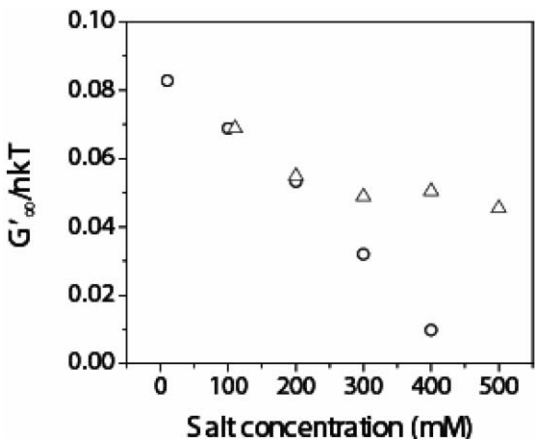

Fig. 5 Effects of salt concentration on the plateau storage modulus of $AC_{10}A$ hydrogels (7% w/v, pH 8.0, 22 °C). Salt concentration is the concentration of phosphate buffer (○) or the sum of the concentration of NaCl and 100 mM phosphate buffer (△).

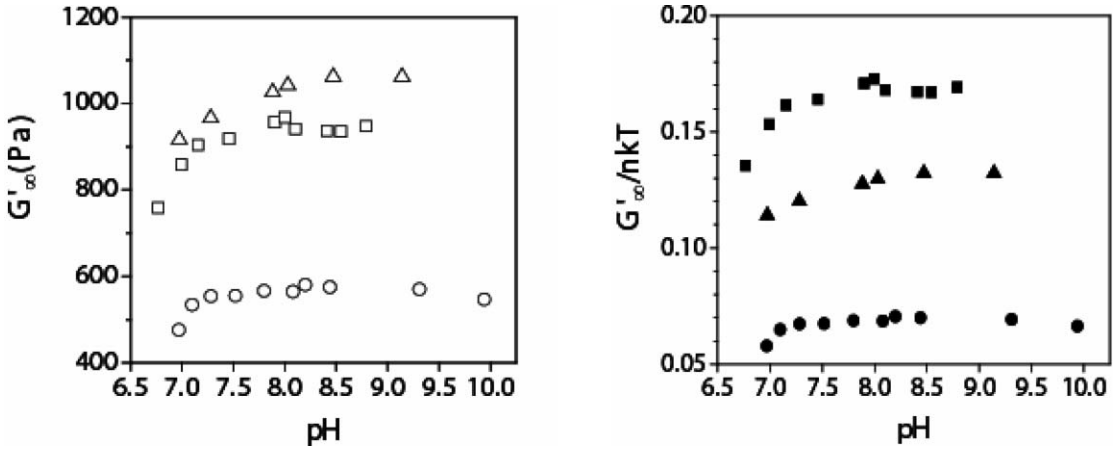

Fig. 6 Plateau storage moduli of $AC_{10}A$ (○, ●); $AC_{26}A$ (□,■); and $AC^*_{18}A$ (△,▲) hydrogels at different pH. (7% w/v, 100 mM phosphate buffer, 22 °C.)

labelled with a donor fluorophore at one end and an acceptor fluorophore at the other ($_{trp}AC_{10}A_{cys}$-CPM) are mixed with a large excess of unlabelled $AC_{10}A$ ($AC_{10}A_{no\text{-}trp}$) chains, efficient FRET should occur only if the labelled chains adopt looped configurations. A 1.25% w/v solution of unlabelled ($AC_{10}A_{no\text{-}trp}$) chains showed negligible emission between 308 and 410 nm (excitation wavelength 300 nm). When chains bearing only donor ($_{trp}AC_{10}A_{cys}$) were added to the $AC_{10}A_{no\text{-}trp}$ solution in a molar ratio of 1 : 25 (the concentration of $AC_{10}A_{no\text{-}trp}$ was 1.01% after mixing), a pronounced emission peak between 308 and 410 nm was observed. When $_{trp}AC_{10}A_{cys}$-CPM was added in similar fashion to the $AC_{10}A_{no\text{-}trp}$ solution, the intensity of the tryptophan emission was reduced by more than 50% compared to that observed in the absence of coumarin (Fig. 8), and strong coumarin emission between 410 and 590 nm was observed. The ratio of the coumarin and tryptophan emission intensities was *ca.* 30. In a control experiment, the donor and acceptor chromophores were added separately (in the form of $_{trp}AC_{10}A_{cys}$ and PEG-CPM, respectively) to the $AC_{10}A_{no\text{-}trp}$ solution. The coumarin emission from this sample (presumably due to direct excitation of coumarin) was *ca.* 10% of that from the mixture of $_{trp}AC_{10}A_{cys}$-CPM and $AC_{10}A_{no\text{-}trp}$ (Fig. 8). The ratio of emission intensities from coumarin and tryptophan was less than 2. These experiments suggest that the predominant molecular mechanism of FRET in $_{trp}AC_{10}A_{cys}$-CPM solutions is the formation of looped configurations. Given that the extent of coumarin labeling in $_{trp}AC_{10}A_{cys}$ is *ca.* 70%, we estimate that the quenching efficiency (E) for labelled chains is 75 ± 4% ($E = [1 - (F_{DA}/F_D)]/f$), where F_{DA} is the donor fluorescence with acceptor present, F_D is the donor fluorescence without acceptor present, and f is the extent of labeling.

Light scattering

To determine the aggregation number of the associative leucine zipper domain using multi-angle static light scattering

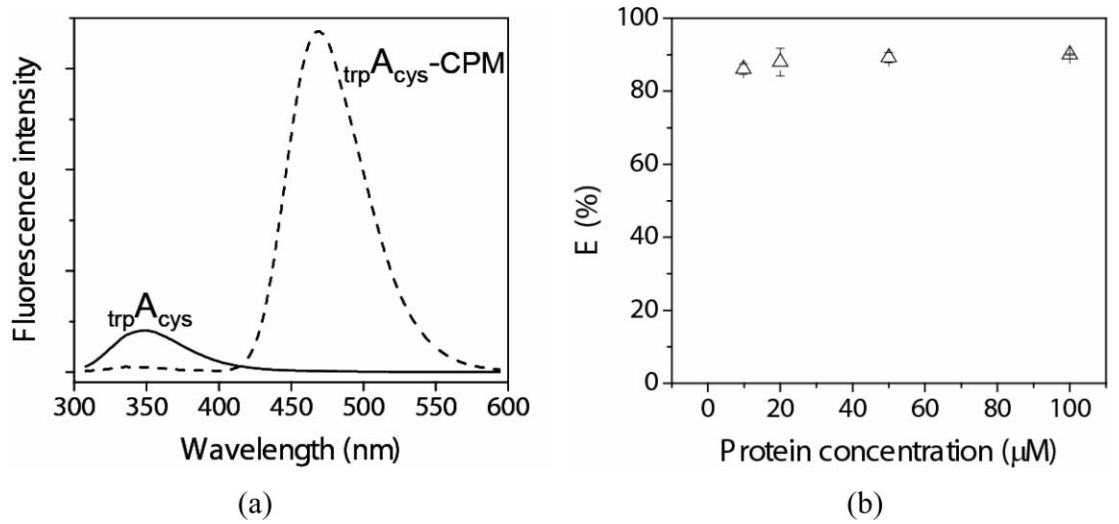

Fig. 7 Probing strand orientation by FRET. (a) Fluorescence emission from $_{trp}A_{cys}$ solutions containing an N-terminal tryptophan in the absence (solid line) or presence (dashed line, $_{trp}A_{cys}$-CPM) of C-terminal coumarin (100 μM protein). The baseline signal from the buffer was subtracted. (b) Fluorescence energy transfer efficiency in $_{trp}A_{cys}$-CPM solutions at various concentrations (100 mM phosphate buffer, pH 7.6, 22 °C).

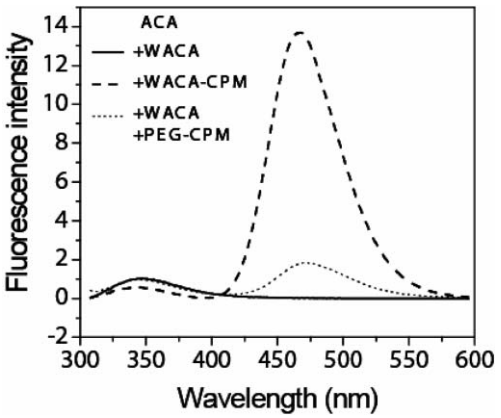

Fig. 8 FRET between distinct chromophores placed at the C- and N-termini of $AC_{10}A$ chains suggests a strong tendency toward loop formation. The fluorescence of the N-terminal tryptophan of ${}_{trp}AC_{10}A_{cys}$ (WACA) is substantially quenched (more than 50%) by the coumarin (CPM) labelled at the C-terminus. The ratio of emission intensities of coumarin and tryptophan is *ca.* 30. In a control experiment where the coumarin is linked to separate polyethylene glycol chains, little tryptophan quenching (less than 5%) is observed. The ratio of emission intensities of coumarin and tryptophan is less than 2. (100 mM phosphate buffer, pH 7.6, 22 °C. The concentration of $AC_{10}A_{no\text{-}trp}$ (ACA) was 1.01% w/v; the molar ratio of $AC_{10}A_{no\text{-}trp}$ to each of other components was 25 : 1. The baseline fluorescence from a 1.01% w/v solution of $AC_{10}A_{no\text{-}trp}$ was subtracted.)

measurements, we engineered the diblock protein AC_{10trp} to capture the steric and electrostatic effects of the C-domain on the association of the A-domains relevant to the $AC_{10}A$ gel. AC_{10trp} solutions were each filtered through a 0.2 μm pore size filter and subjected to light scattering measurements. The data were analyzed by Zimm plot analysis. The scattering curves are not linear, as suggested by a first order fit. A better description of the data is achieved with a second order fit, revealing an average molar mass of $(6.79 \pm 0.10) \times 10^4$ Da, which is only 4.8% greater than the value obtained by the linear treatment ($(6.47 \pm 0.10) \times 10^4$ Da). This molar mass is close to the expected molar mass for tetramers (6.52×10^4 Da) (Fig. 9). Tetrameric association of the leucine zipper domain was suggested previously by Kennedy *et al.* on the basis of analytical ultracentrifugation and small-angle X-ray scattering (SAXS) studies.[22] In particular, data from small-angle X-ray scattering studies performed on $AC_{10}A$ solutions at concentrations as high as 7% w/v (*ca.* 6.3 mM leucine zipper) fit well to a cylindrical model for tetrameric helical bundles with the following dimensions: length 63 Å, radius 13.6 Å, and a 1 Å axial pore. Thus, our light scattering results on AC_{10} diblocks, taken together with prior literature on the A domain alone and $AC_{10}A$ hydrogels, indicate that the A domain predominantly forms tetrameric aggregates at concentrations ranging from *ca.* 10 μM to 6 mM.

Zimm plot analysis revealed a negative second virial coefficient (A_2) for tetrameric aggregates of AC_{10}. The central portion of these tetramers, in which the helical zippers are side-by-side, is *ca.* 6.3 nm long and 2.8 nm wide. Unlike a familiar micelle, four C_{10} domains (radius of gyration *ca.* 2.5 nm, two at each end of the bundle of four zippers) cannot form a corona that covers the entire bundle of leucine zippers.

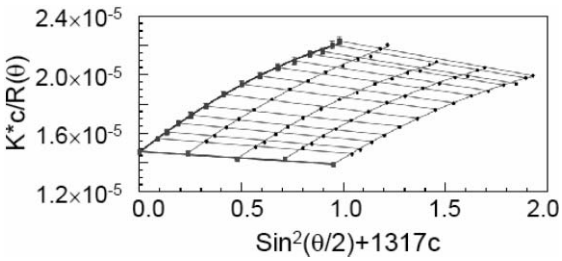

Fig. 9 Zimm plot of multi-angle light scattering intensities from AC_{10trp} solutions. Concentrations of the solutions subjected to measurements were 11.0 μM, 22.0 μM, 33.0 μM and 44.0 μM (100 mM phosphate buffer, pH 7.6, 22 °C). The average molar mass is $(6.47 \pm 0.10) \times 10^4$ Da, suggesting tetrameric association (the molar mass of monomer AC_{10trp} is 1.63×10^4 Da).

Therefore, even if the C_{10} chains themselves have $A_2 > 0$, the AC_{10} tetramers have $A_2 < 0$ due to the exposed area of the leucine zipper bundles.

Quasi-elastic light scattering measurements for C_{10trp} solutions (pH 10.0) were performed on WyattQELS and BI-9000AT digital autocorrelators to reveal the dimensions of the C_{10} domain. Samples were filtered through 0.2 μm filters prior to measurements on WyattQELS. A small tail at time longer than 60 μs was observed. When samples were filtered through 0.02 μm filters, the signal fell to zero by 60 μs, suggesting that trace amounts of foreign particles existed when samples were filtered through 0.2 μm filters. Large objects did not reappear after filtration using 0.02 μm pore filters; therefore, we concluded that they were not formed from the protein itself. Since extremely dilute large particles could not alter the short time correlations, the correlation function on the time range from 1 to 60 μs was analyzed on the basis of the CONTIN algorithm and revealed a mean hydrodynamic radius (R_H) of 20 Å.

The observed R_H is slightly greater than the size expected for a denatured polypeptide under θ conditions, suggesting that water is somewhere between a θ solvent and a good solvent for the (AGAGAGPEG) sequence. For denatured proteins having more than 50% glycine in a θ solvent, the characteristic ratio $\langle R^2 \rangle / n_p l_p^2$ is 2.0–3.2,[23] where $\langle R^2 \rangle$ is mean square end-to-end distance; n_p is the number of peptide bonds; and l_p is the distance between adjacent α-carbon atoms, *ca.* 3.8 Å. Since the mole fraction of glycine in the C_{10} domain is close to 50% and circular dichroism analysis suggests that it does not have significant secondary structure,[24] its average end-to-end distance is predicted to be

$$\sqrt{\langle R^2 \rangle} \approx 51 - 64 \text{ Å}$$

under θ conditions. This is close to the value of $\langle R^2 \rangle$ estimated from the measured R_H. Since

$$\sqrt{\langle R^2 \rangle} \Big/ R_g \approx \sqrt{6}$$

,[25–27] where R_g is the radius of gyration, and R_g/R_H for solutions above the θ temperature is *ca.* 1.2–1.5,[28,29] we estimate that the C_{10} domain has

$$\sqrt{\langle R^2 \rangle} \approx 59 - 73 \text{ Å}$$

Electrophoretic assessment of parallel *vs.* antiparallel leucine zipper association

The orientation of leucine zipper strands in aggregates was also examined by electrophoresis of mixtures of $_{cys}$A and $C_{10}A_{cys}$, which bear cysteine residues at the N- and C-termini, respectively. The antiparallel orientation brings these residues into proximity, and allows linkage through thiol–disulfide exchange when a redox buffer is added. The linked heterodimers (molar mass 24 989 Da) can be resolved from the homodimers (masses 8394 Da and 16 595 Da, respectively) by denaturing PAGE. When solutions of $_{cys}$A and $C_{10}A_{cys}$ at pH 8.0 (where the zipper exchange time is *ca.* 100 s (ref. 12)) were co-incubated for 48 h, then exposed to redox buffer for 3 h, linked heterodimers were observed (Fig. 10). A band located between the $C_{10}A_{cys}$ homodimer (band 1) and the $C_{10}A_{cys}$ monomer (band 3) was observed in mixed solutions, but not in solutions of either protein alone, suggesting antiparallel strands are present in the aggregates. Densitometry analysis (NIH ImageJ[30]) revealed that the molar ratio of heterodimers to $C_{10}A_{cys}$ homodimers (band 1) is 0.84 ± 0.07, suggesting that the majority of the tetrameric aggregates contain antiparallel leucine zipper strands.

Discussion

Network topology governs the stiffness of $AC_{10}A$ gels

The low values of G'_∞/nkT (less than 13%) under all conditions examined here suggest that the elastically effective chain fraction is low in $AC_{10}A$ hydrogels (Fig. 3–5). On a molecular level, the most likely explanation is that $AC_{10}A$ chains tend to form a substantial fraction of looped configurations that do not contribute to network elasticity. The tendency of $AC_{10}A$ chains to form loops is supported by the significant quenching of the fluorescence of an N-terminal tryptophan by a C-terminal coumarin (Fig. 8). Loops in $AC_{10}A$ hydrogels and the consequent low plateau storage moduli are governed by the structural features of the central and terminal domains, including the aggregation number of the leucine zipper domain, parallel *vs.* antiparallel leucine zipper association, and the dimensions of the midblock.

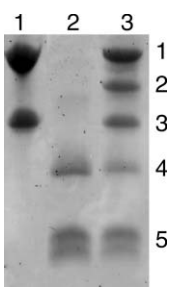

Fig. 10 Electrophoresis of mixtures of $_{cys}$A and $C_{10}A_{cys}$ revealed antiparallel leucine zipper strands in aggregates. Lane: 1. $C_{10}A_{cys}$; 2. $_{cys}$A ; 3. mixture of $_{cys}$A and $C_{10}A_{cys}$ with addition of redox buffer. Band: 1. dimer of $C_{10}A_{cys}$ linked by a disulfide bond; 2. $_{cys}$A and $C_{10}A_{cys}$ heterodimer linked by a disulfide bond; 3. monomer $C_{10}A_{cys}$; 4. dimer of $_{cys}$A linked by a disulfide bond; 5. monomer $_{cys}$A. In lane 3, the molar ratio of the protein in band 2 to that in band 1 is estimated to be $84 \pm 7\%$ on the basis of densitometry analysis using NIH ImageJ (assuming identical staining for different domains).

Compared to conventional hydrophobic associative groups (alkyl or fluoroalkyl type) that lead to transient networks, leucine zipper domains are characterized by small aggregation numbers. Naturally occurring leucine zipper domains oligomerize into dimers, trimers, tetramers or pentamers.[31,32] Higher order aggregates have not been reported, probably due to the narrow hydrophobic face on each strand. Tetrameric association of leucine zipper A was revealed by multi-angle static light scattering experiments on AC_{10trp} solutions (Fig. 9), in accord with prior findings of Kennedy *et al.*[22] This small aggregation number makes the elastically effective chain fraction very sensitive to intramolecular association, contributing to the exceptionally low plateau storage modulus of $AC_{10}A$ networks. For example, an aggregate that contains one looped chain simply links two other chains into one elastically effective chain, and therefore three chains are consumed to produce only one elastically effective strand.

The compact size of the midblock compared to the distance between aggregates increases the tendency to form loops. Quasi-elastic light scattering of a C_{10trp} solution revealed that the mean hydrodynamic radius of the C_{10} domain is 20 Å, corresponding to a root-mean-square end-to-end distance of 59–73 Å. The center-to-center distance between leucine zipper aggregates in a 7% w/v $AC_{10}A$ solution is *ca.* 100 Å (estimate based on tetramers placed on the corners of a cube). To avoid the energy penalty for stretching the midblock, the chains tend to form loops.

The ability of the midblock to form loops depends on the ability of the leucine zipper end blocks to adopt antiparallel arrangements in the tetramer, which in turn depends on the specific amino acid sequence selected for the leucine zipper. Since the length of the present leucine zipper helices is *ca.* 65 Å, formation of a C_{10} loop with its ends at opposite ends of a tetramer (*i.e.*, parallel orientation of its leucine zipper end blocks (N→C/N→C)) is entropically unfavorable. The hypothesis that the loop fraction is substantial in $AC_{10}A$ networks is only plausible if the A domains can accommodate antiparallel configurations (N→C/C→N) in tetrameric aggregates so that the midblock is not stretched. Therefore, it is particularly significant that antiparallel configurations were evident, both by FRET between specifically labelled A chains (Fig. 7) and by the formation of heterodimers of $_{cys}A/C_{10}A_{cys}$ in thiol–disulfide exchange experiments (Fig. 10).

Conditions that expand the midblock and decrease inter-aggregate distance disfavor loops

The observed effects of concentration, pH and salt on G'_∞ are interesting and, in the cases of pH and salt, counter-intuitive; however, they can be readily understood in view of the importance of midblock chain dimensions for the loop-to-bridge ratio. With increasing concentration, if the topology of the network (*i.e.* the loop-to-bridge ratio) did not change, G'_∞/nkT would be constant. Instead, G'_∞/nkT increases strongly with concentration (Fig. 3): as the average distance between leucine zipper aggregates decreases, the penalty for

stretching the midblock to span aggregates becomes less severe, so the loop-to-bridge ratio decreases, leading to an increase in G'_∞/nkT. This behavior is analogous to the change in network topology with concentration in conventional associative polymers.[33]

The nonmonotonic effect of pH on G'_∞ (Fig. 4 and 5) at first seems surprising. With increasing pH, leucine zipper association becomes weaker, as indicated by faster strand exchange and network relaxation.[12] Destabilized leucine zipper association could decrease network connectivity, leading to the expectation that materials either retain constant rigidity or even become softer as pH increases. The increase in modulus as pH increases from 7 to 8 (Fig. 4) must originate instead from changes in the midblock, a random coil polyelectrolyte whose charge density increases with increasing pH. In chemically crosslinked polyelectrolyte networks that have fixed topology, the storage modulus decreases when electrostatic repulsion among chain segments increases,[34,35] because less external energy (stress) is required to stretch the chain to the same extent (strain). The atypical trend exhibited by $AC_{10}A$ networks can only be explained through changes in topology.

To examine the effect of pH on the charge density of the midblock, a histidine-tag-free C_{10trp} solution was titrated. Although the pK_a value of an isolated glutamic acid residue is 4.4, titration of the C_{10} solution revealed a buffering regime between pH 7 and 8, suggesting that deprotonation of the glutamic acid residues in the midblock extends into this pH regime. This change in pK_a lies within the range of pK_a shifts induced by hydrophobic and charged residues in proximity.[36] Thus, the pH range in which G'_∞ increases coincides with an increase in electrostatic repulsion in the midblock due to the increase in the number of negatively charged glutamic acid residues. The increased electrostatic repulsion results in an expansion in the midblock, which reduces the loop-to-bridge ratio and consequently increases G'_∞/nkT.

The effects of ionic strength can similarly be understood in terms of the conformation of the polyelectrolyte midblock. Coil dimensions of a polyelectrolyte decrease as ionic strength increases due to both screening of electrostatic repulsion and increasing persistent length and rigidity.[37] Thus, as ionic strength increases, the C_{10} domain becomes more compact, causing the modulus to decrease (Fig. 5), consistent with reducing the loop-to-bridge ratio.

Understanding network topology provides molecular design principles for new materials

Understanding structural features of the building blocks of $AC_{10}A$ and their effects on material properties provides molecular design guidelines to increase material rigidity.[10] Here we present the example of engineering the midblock. Based on the importance of network topology, we anticipated that midblocks of great length or higher charge density would favor bridges over loops and lead to networks exhibiting plateau storage moduli larger than those of $AC_{10}A$ hydrogels. Two new triblock proteins were synthesized, one with the midblock length more than doubled ($AC_{26}A$) and one with charge density (frequency of glutamic acid, E, residues) nearly doubled ($AC^*_{18}A$). As expected, both assembled into hydrogels that had G'_∞ values roughly twice that of $AC_{10}A$ hydrogels (Fig. 6). Although increasing the chain length between crosslinking points generally decreases the elasticity of network materials, the plateau storage moduli of $AC_{10}A$ and $AC_{26}A$ hydrogels show an opposite trend. This is because the plateau storage moduli of these hydrogels are determined by two competing factors: the total chain number density and the elastically effective chain fraction. When the midblock C_{10} is replaced by C_{26}, the increase in the fraction of elastically effective chains overcomes the decrease in the chain number density and leads to a greater plateau storage modulus. As noted above, in covalent polyelectrolyte networks, increasing charge density decreases gel modulus. Here the opposite trend is observed due to the increase in the effective chain fraction for C^*_{18} relative to C_{10}.

Conclusions

Network topology plays a dominant role in determining the storage modulus of $AC_{10}A$ hydrogels. $AC_{10}A$ chains have a strong tendency to form loops due to the compact random coil midblock and the ability of the leucine zipper A domain to adopt antiparallel arrangements in aggregates. Furthermore, loop formation has unusually pronounced effects on G'_∞ because of the small aggregation number of the leucine zipper domain (tetrameric association). Understanding the importance of the loop-to-bridge ratio in the network provides a unified explanation of the intriguing effects of concentration, pH and ionic strength on G'_∞. Physical insights into these structure–property relationships led to successful design strategies to control material properties through careful molecular engineering. In particular, contrary to the behavior of conventional gels, the plateau storage modulus increased when the midblock C_{10} was replaced by new polypeptides with either greater contour length or higher charge density.

Acknowledgements

The authors acknowledge the NSF Center for the Science and Engineering of Materials for financial support.

References

1 K. Almdal, J. Dyre, S. Hvidt and O. Kramer, *Makromol. Chem., Macromol. Symp.*, 1993, **76**, 49–51.
2 W. A. Petka, J. L. Harden, K. P. McGrath, D. Wirtz and D. A. Tirrell, *Science*, 1998, **281**(5375), 389–392.
3 L. Y. Koo, D. J. Irvine, A. M. Mayes, D. A. Lauffenburger and L. G. Griffith, *J. Cell Sci.*, 2002, **115**(7), 1423–1433.
4 J. S. Tjia and P. V. Moghe, *Tissue Eng.*, 2002, **8**(2), 247–261.
5 D. Ilic, E. A. C. Almeida, D. D. Schlaepfer, P. Dazin, S. Aizawa and C. H. Damsky, *J. Cell Biol.*, 1998, **143**(2), 547–560.
6 A. Engler, L. Bacakova, C. Newman, A. Hategan, M. Griffin and D. Dischery, *Biophys. J.*, 2004, **86**(1), 617–628.
7 B. Geiger and A. Bershadsky, *Curr. Opin. Cell Biol.*, 2001, **13**(5), 584–592.
8 C. M. Lo, H. B. Wang, M. Dembo and Y. L. Wang, *Biophys. J.*, 2000, **79**(1), 144–152.
9 J. Y. Wong, A. Velasco, P. Rajagopalan and Q. Pham, *Langmuir*, 2003, **19**(5), 1908–1913.
10 W. Shen, K. C. Zhang, J. A. Kornfield and D. A. Tirrell, *Nat. Mater.*, 2006, **5**(2), 153–158.

11 W. Shen, J. A. Kornfield and D. A. Tirrell, Dynamic properties of artificial protein hydrogels assembled through aggregation of leucine zipper peptide domains, *Macromolecules*, accepted.
12 W. Shen, Structure, dynamics, and properties of artificial protein hydrogels assembled through coiled-coil domains, *PhD Dissertation*, California Institute of Technology, Pasadena, CA, 2005.
13 W. Shen, R. G. H. Lammertink, J. K. Sakata, J. A. Kornfield and D. A. Tirrell, *Macromolecules*, 2005, **38**(9), 3909–3916.
14 Y. M. Liou, M. J. Jiang and M. C. Wu, *J. Biochem.*, 2002, **132**(2), 317–325.
15 M. B. Huglin, *Light scattering from polymer solutions*, Academic Press, London, New York, 1972.
16 A. Saghatelian, Y. Yokobayashi, K. Soltani and M. R. Ghadiri, *Nature*, 2001, **409**(6822), 797–801.
17 J. D. Ferry, *Viscoelastic properties of polymers*, Wiley, New York, 1980.
18 B. W. van der Meer, G. Coker, III and S.-Y. S. Chen, *Resonance energy transfer: theory and data*, VCH, New York, 1994.
19 M. A. Trakselis, R. M. Roccasecca, J. S. Yang, A. M. Valentine and S. J. Benkovic, *J. Biol. Chem.*, 2003, **278**(50), 49839–49849.
20 R. A. Garcia, C. E. Forde and H. A. Godwin, *Proc. Natl. Acad. Sci. U. S. A.*, 2000, **97**(11), 5883–5888.
21 R. S. Hodges, *Biochem. Cell Biol.*, 1996, **74**(2), 133–154.
22 S. B. Kennedy, K. Littrell, P. Thiyagarajan, D. A. Tirrell and T. P. Russell, *Macromolecules*, 2005, **38**(17), 7470–7475.
23 W. L. Mattice and L. Mandelke, *Biochemistry*, 1971, **10**(10), 1934–1942.
24 W. A. Petka, Reversible gelation of genetically engineered macromolecules, *PhD Dissertation*, University of Massachusetts Amherst, Amherst, MA, 1997.
25 M. K. Kosmas, *J. Phys. A: Math. Gen.*, 1981, **14**(10), 2779–2788.
26 P. J. Flory, *Principles of polymer chemistry*, Cornell University Press, Ithaca, N.Y., 1953.
27 J. des Cloizeaux and G. Jannink, *Polymers in solution: their modelling and structure*, Clarendon Press, Oxford, Oxford University Press, New York, 1990.
28 Y. Oono and M. Kohmoto, *J. Chem. Phys.*, 1983, **78**(1), 520–528.
29 M. Doi, *Introduction to polymer physics*, Clarendon Press, Oxford, Oxford University Press, New York, 1996.
30 W. Rasband, *NIH ImageJ*, National Institute of Mental Health, Bethseda, Maryland, USA, 1997.
31 V. N. Malashkevich, R. A. Kammerer, V. P. Efimov, T. Schulthess and J. Engel, *Science*, 1996, **274**(5288), 761–765.
32 P. B. Harbury, T. Zhang, P. S. Kim and T. Alber, *Science*, 1993, **262**(5138), 1401–1407.
33 T. Annable, R. Buscall, R. Ettelaie and D. Whittlestone, *J. Rheol.*, 1993, **37**(4), 695–726.
34 M. Rubinstein, R. H. Colby, A. V. Dobrynin and J. F. Joanny, *Macromolecules*, 1996, **29**(1), 398–406.
35 A. V. Dobrynin, R. H. Colby and M. Rubinstein, *Macromolecules*, 1995, **28**(6), 1859–1871.
36 D. W. Urry, *J. Phys. Chem. B*, 1997, **101**(51), 11007–11028.
37 M. Schmidt, *Macromolecules*, 1991, **24**(19), 5361–5364.